*Volume 2, Number 2: 16-26, October 2004*

International Journal of
Vascular Biomedical Engineering

# Simulation of Cardiovascular System for an Optimal Sodium Profiling in Hemodialysis

K M Lim[1], B G Min[2] and E B Shim[3¶]

[1] *Interdisciplinary Program in Biomedical Engineering Major, Seoul National University, Seoul, Korea*
[2] *Department of Biomedical Engineering, College of Medicine, Seoul National University, Seoul, Korea*
[3] *Department of Mechanical engineering, Kangwon National University, Chuncheon, Korea*

## Abstract

The object of this study is to develop a mathematical model of the hemodialysis system including the mechanism of solute kinetics, water exchange and also cardiovascular dynamics. The cardiovascular system model used in this study simulates the short-term transient and steady-state hemodynamic responses such as hypotension and disequilibrium syndrome (which are main complications to hemodialysis patients) during hemodialysis. It consists of a 12 lumped-parameter representation of the cardiovascular circulation connected to set-point models of the arterial baroreflexes, a kinetic model (hemodialysis system model) with 3 compartmental body fluids and 2 compartmental solutes. We formulate mathematically this model in terms of an electric analog model. All resistors and most capacitors are assumed to be linear. The control mechanisms are mediated by the information detected from arterial pressoreceptors, and they work on systemic arterial resistance, heart rate, and systemic venous unstressed volume. The hemodialysis model includes the dynamics of urea, creatinine, sodium and potassium in the intracellular and extracellular pools as well as fluid balance equations for the intracellular, interstitial, and plasma volumes. Model parameters are largely based on literature values. We have presented the results on the simulations performed by changing some model parameters with respect to their basal values. In each case, the percentage changes of each compartmental pressure, heart rate (HR), total systemic resistance (TSR), ventricular compliance, zero pressure filling volume and solute concentration profiles are represented during hemodialysis.

Key Words : Cardiovascular system, Hemodialysis system, Baroreflex control, Three compartment model of body fluid

## Introduction

Clinical tolerance to hemodialysis is still a problem, although artificial materials and machines have been continuously improved. The main complications are symptomatic hypotension and disequilibrium syndrome which are caused by osmotic unbalance among intracellular, interstitial and plasma compartments. Although these phenomena are of the greatest clinical importance, the origin and underlying mechanisms are still insufficiently understood. An plausible cause of hypotension and disequilibrium syndrome among what we have known so far is the decrease in intravascular volume resulting from ultrafiltration (UF). Moreover, the changes in plasma osmolality induced by dialysis may result in inter-compartmental fluid shifts[1]. In order to prevent these complications and understand the mechanism, it is necessary to develop a mathematical model of hemodialysis and cardiovascular system to predict hemodynamic response during hemodialysis treatment quantitatively.

There have been many simulation studies of cardiovascular system with baroreflex autoregulation[2-5] and hemodialysis systems which describes either the volume fluid shift in body compartments or solute kinetics[6-10]. The mathematical models of hemodialysis system were proposed to predict volume changes by considering a 2-pool kinetic model of water, urea, and sodium[3]. More comprehensive mathematical models,

¶Dep. of Mech. & Mechatronics Eng., Kangwon National Univ., Chuncheon, Kangwon-do, Korea
E-mail: ebshim@kangwon.ac.kr

including a 3-pool kinetic model, have also been proposed[8-10]. In the cardiovascular system model for hemodynamic response to some environmental changes, Boyers and co-workers[11] implemented a seven-compartment steady-state model coupled with the arterial baroreflex system. Croston and Fitzjerrell[12] devised a 28-compartment lumped-parameter model: arterial, venous, and cardiac compartments are modeled in terms of coupled ordinary differential equations that describe the dynamics of the system. Heldt et al[13] have considered 12 lumped parameter model, and baroreflex regulation system model to simulate hemodynamic response to different environmental conditions. Particularly, the response of the cardiovascular system to hemodialysis has been the focus of several mathematical models. Ursino et al.[8] have reported the prediction of hypotension using a combined model which includes 8 compartments, baroreflex autoregulation system and hemodialysis system. Since the model was too simple in peripheral circulation, his model could not describe the detailed hemodynamics. Therefore, we have combined the previous model of Ursino[7] for hemodialysis system with the previous model[13] for cardiovascular system to simulate hemodynamic response to hemodialysis treatment. The present model includes 12 lumped

compartments, baroreflex regulation system, 3 compartment model of body fluid and 2 compartment model of solute kinetics. Using this model, we predict the solute kinetics and cardiovascular response to hemodialysis

## Model Description

In this section we first describe the hemodynamic aspects of the cardiovascular system, including pressure losses, blood volume storage, and activity of the heart. In the second, the short-term mechanisms are introduced. Finally we analyze fluid exchange between body compartments and the dynamics of the main solutes. The set of differential equations are solved numerically on a personal computer using a Runge-Kutta method with an adjustable step length.

### The Cardiovascular System Model

The hemodynamic model is mathematically formulated in terms of an electric analog model. All resistors and most capacitors are assumed to be linear. These assumptions lead to governing 1st order differential equations. Fig. 1 shows an example of the compartments. The entire model, as shown in Fig. 2, is described mathematically by 13 first-order differential equations with the model parameters in Table 1.

The peripheral circulation is divided into upper body, renal, splanchnic, and lower extremity sections; the intrathoracic superior and inferior vena cava and extrathoracic (Abdominal) vena cava are separately identified. Each of the model compartments is represented by a linear resistance (R) and a capacitance (C) that can be either linear, nonlinear, or time varying The pumping action of the heart is realized by varying the right and left ventricular elastances according to a predefined function of time ($E_r(t)$ and $E_l(t)$, respectively).

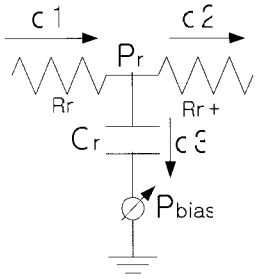


Figure 1 Single-compartment circuit representation. P, pressure; R, resistance; C, compliance; q1, q2, and q3, blood flow rates as indicated; n-1, n, n+1, compartment indexes; $P_{bias}$, external pressure.

Table 1. Cardiovascular system parameters

| | Resistance (PRU) | ZPFV (mL) | Compliance (mL/mmHg) |
|---|---|---|---|
| Right ventricle | 0.003 | 50 | 1.2-20 |
| Pulmonary arteries | 0.08 | 90 | 4.3 |
| Pulmonary veins | 0.01 | 490 | 8.4 |
| Left Ventricle | 0.006 | 50 | 0.4-10 |
| Systemic arteries | | 715 | 2.0 |
| Upper body 1 | 3.9 | 650 | 8 |
| Upper body 2 | 0.23 | | |
| Kidney 1 | 4.1 | 150 | 15 |
| Kidney 2 | 0.3 | | |
| Splanchnic 1 | 3.0 | 1,300 | 55 |
| Splanchnic 2 | 0.18 | | |
| LowerLimbs 1 | 3.6 | 350 | 19 |
| LowerLimbs 2 | 0.3 | | |
| Abdominal veins | 0.01 | 250 | 25 |
| Inferior vena cava | 0.015 | 75 | 2 |
| Superior vena cava | 0.06 | 10 | 15 |

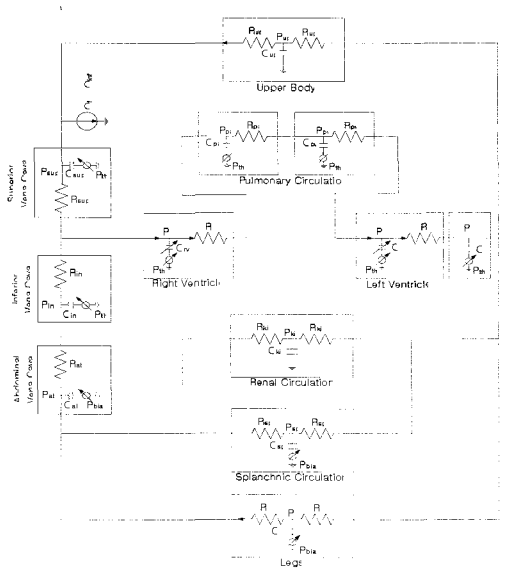


Figure 2. Circuit diagram of the hemodynamic system. $L_v$, Left ventricle; a, arterial; up, upper body; kid, kidney; sp, splanchnic; ll, lower limbs; ab, abdominal vena cavea; inf , inferior vena cava; sup, superior vena cava; rv, right ventricle; p, pulmonary; pa, pulmonary artery; pv, pulmonary vein; ro, right ventricular outflow; lo, left ventricular outflow; th, thoracic; bias, as defined in Fig 1.

$$E(t)=\begin{cases} E_{dias}+\dfrac{E_{sys}-E_{dias}}{2}\left\{1-\cos\left(\pi\dfrac{t}{0.3\sqrt{T(n-1)}}\right)\right\} & 0\le t\le T_s \\ E_{dias}+\dfrac{E_{sys}-E_{dias}}{2}\left\{1+\cos\left(2\pi\dfrac{t-0.3\sqrt{T(n-1)}}{0.3\sqrt{T(n-1)}}\right)\right\} & T_s\le t\le\dfrac{3}{2}T_s \\ E_{dias} & \dfrac{3}{2}T_s\le t\le T(n) \end{cases} \quad (1)$$

$E_{dias}$ and $E_{sys}$ represent the end-diastolic and end-systolic elastance values, respectively, T(i) denotes the cardiac cycle length of the $i^{th}$ beat, and t denotes time measured with respect to the onset of ventricular contraction. Atria are not represented; their function is, however, partially absorbed into the function of adjacent compartments. Diodes represent valves that ensure unidirectional flow through the ventricles and parts of the venous system. A time-varying pressure source, $P_{th}$, simulates changing transmural pressure across the intrathoracic compartments.

## The Baroreflex System Model

We have adopted a previously reported regulatory set-point model of the arterial baroreflex that aims at maintaining mean arterial blood pressure constant by dynamically adjusting heart rate, peripheral resistance, venous zero-pressure filling volume, and right and left end-systolic cardiac capacitances[13] (see Fig. 3).

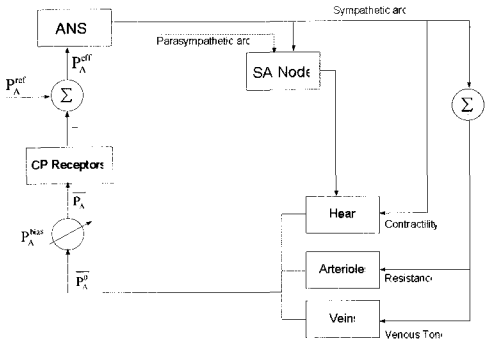


Figure 3. Diagrammatic representation of the reflex model. CS, carotid sinus ANS, autonomic nervous system; SA, sinoatrial; sigma, summation. See text for definitions of pressure (P) symbols.

Briefly, the predefined set-point pressures are subtracted from locally sensed blood pressures to generate error functions that are relayed to the autonomic nervous system, where the error signals are rescaled. These error signals subsequently dictate the efferent activity of the reflex model such that the error signals approach zero over the next computational steps. The input variables to the control system are mean arterial pressure ($P_A$) for the arterial baroreflex as substitutes for carotid sinus pressure ($P_{cs}$). The respective error signal is generated by subtracting predefined set-point value ( $p_A^{ref}$ ) from these input variable and rescaling by and arctangent to generate effective blood pressure deviation ( $p_A^{eff}$ ).

$$p_A^{eff}=18\tan^{-1}\left[\frac{P_A-P_A^{ref}}{18}\right] \quad (2)$$

To account for differences in timing of the reflex responses, the respective effective blood pressure deviations are weighted by impulse response functions that are characteristic of a parasympathetic p(t) or sympathetic s(t) response. (see Fig 3). The model thus provides for a rapid (~0.5 – 1 s) sympathetic reflex response. A 30-second running history of the effective pressures is used to compute instantaneous effector values by convolution with the appropriate effector

specific impulse responses as the following example of R-R interval (I) feedback shows

$$I(t) = I_0 + \int_{k=0}^{k=30} P_A^{eff}(t-k)\cdot[\beta\cdot p(k) + \gamma\cdot s(k)]dk \qquad (3)$$

The contribution of the arterial baroreflex to the instantaneous R-R interval at time t [I(t)] is computed by adding a dynamically computed contribution to the baseline value, $I_0$. The impulse response functions, p(k) and s(k), are multiplied by the static gain values, $\beta$ and $\gamma$, for the respective reflex arcs.

## The Hemodialysis System Model : Water exchange (3 compartment model)

In this model, we consider 3 compartments (Fig. 4) that represent the intracellular fluid (in), interstitial fluid (is), and plasma (pl), respectively. Water exchange between the intracellular and interstitial compartments is mainly a result of an osmotic pressure difference at the cellular membrane. This pressure difference is determined by the change of the solute concentrations in the extracellular and intracellular pools and by the contributions of the heavy molecules (mainly glucose and proteins in the interstitial compartment) that do not cross cellular membrane. Fluid exchange from the interstitial fluid to the plasma depends on the oncotic and hydraulic pressure gradients at the arteriolar and venular capillaries. The oncotic pressures in the plasma and the interstitial fluid are computed by means of the Landis-Pappenheimer equations under the assumption that proteins do not cross either the capillary wall or the dialyzer membrane. The hydraulic pressure in the interstitial fluid is computed as a function of the interstitial fluid volume, assuming a constant tissue elastance.

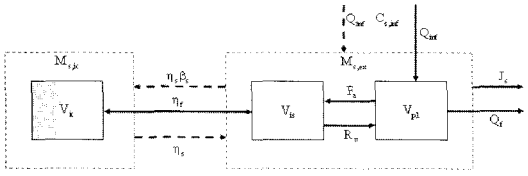

Figure 4 The compartment models used for the description of body fluid exchange and solute kinetics are represented. The dotted lines show the 2 compartment model for the kinetics of the genetic solute s (s is either urea, potassium, or sodium). The solid lines indicate the 3 compartment model of body fluid exchange. $M_{s,ic}$ and $M_{s,ex}$ are the solute masses in the extracellular and intracellular spaces; $K_s$ and $[beta]_s \cdot K_s$ are the mass transfer coefficients of solute s between the intracellular and extracellular compartments; $V_{ic}$, $V_{is}$, and $V_{pl}$ are the intracellular, interstitial, and plasma volumes; $V_{ex}$, the sum of $V_{is}$ and $V_{pl}$, is the extracellular volume; $Q_{inf}$ and $Q_F$ are the infusion rate of the replacement fluid and the ultrafiltration rate; $C_{s,inf}$ is the concentration of solute s in the replacement fluid; $J_s$ is the rate of solute removal across the dialyzer; $R_v$ is the fluid reabsorption rate at the venular capillaries; $F_a$ is the fluid filtration rate at the arterial capillaries; and $K_f$ is the osmotic ultrafiltration coefficient at the cellular membrane. (referenced by Ursino et. al.1997)

## The Hemodialy System Model : Solute kinetics (2 compartment model)

In contrast, the concentrations of the main solutes are assumed to be equal in plasma and the interstitial fluid and so only 2 compartments are considered when describing solute kinetics. In the model of solute kinetics, 5 substances are considered: potassium and sodium, the major determinants of osmolarity at the cellular membrane, and urea, creantine and $HCO_3$. Solute flow rate from the intracellular to the extracellular pool is assumed to increase linearly with the concentration in the intracellular fluid and to decrease linearly with the concentration in the extracellular one. In sodium and potassium dynamics, the mass transfer coefficients include both passive and active transport while only diffusive transport is considered in urea dynamics. As shown in Fig. 4, the rate of exchange of solute in the extracellular compartment results from three distinct contributions, two positive ones that represent the amount of solute coming from the intracellular compartment and the amount injected into plasma through the replacement fluid and a negative one that represents the amount of solute crossing the dialyzer.

Injection of the replacement fluid is used during hemofiltration. Solute flow through the dialyzer includes both convective and diffusive transports according to the equations proposed by Sargent and Gotch[6].

## Result

### CARDIOVASCULAR SYSTEM BASAL SIMULATION

Representative simulated pressure and volume wavforms are shown in Figure 5 (left ventricular, right

ventricular, arterial, pulmonary artery and pulmonary vein). All major hemodynamic parametners generated by the model are within the range of what is considered physiologically normal in the general population[13].

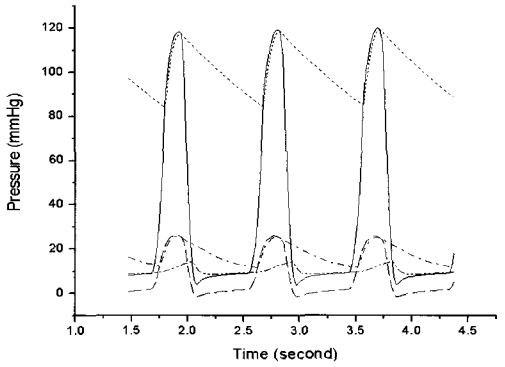


(a)

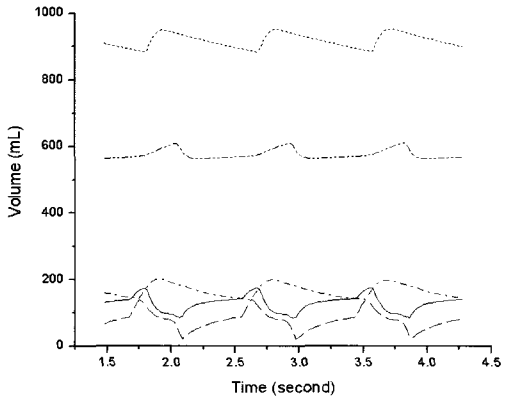


(b)

Figure 5 Simulated pressure and volume wave-forms. (straight: left ventricle, dashed line: right ventricle, dotted line: artery, dash dot line: pulmonary artery, dash dot dot: pulmonary vein)

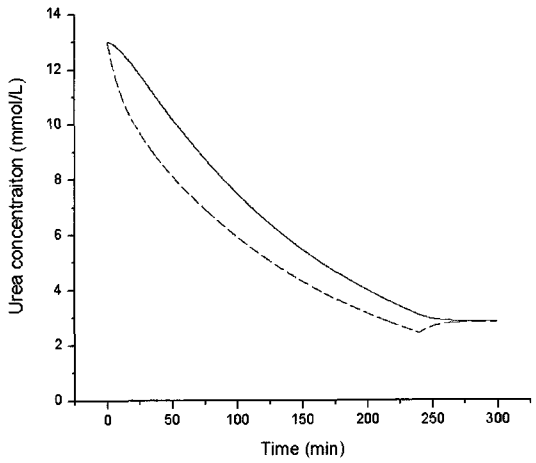


(a)

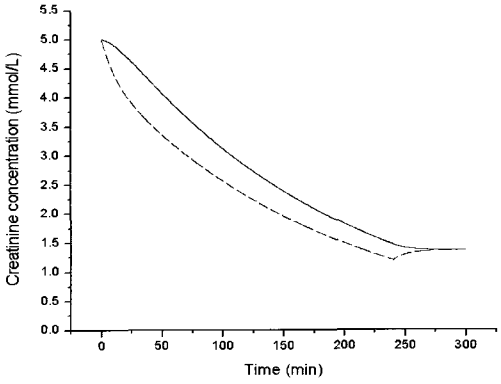


(b)

Figure 6 Time courses of Urea (a) and creatinine (b) concentratration during 4 hour hemodialyls treatment and 1 hour for observation (hyponatric dialysate: 130 mEq/L of dialysate Na+ concentration and 140 mEq/L of plasma Na+ concentration ).

## Hemodialysis System Simulation

We simulated a hemodialysis session with 0.5L/hr UF rate for 4 hours. All simulated sessions were calculated for an adult of 70kg at dry weight with an excess water volume, an initial plasma urea and creatinine concentrations of 2L, 13 mmol/L and 5 mmol/L, respectively. Initial plasma $Na^+$ and $K^+$ were 140mEq/L and 5.5 mEq/L, respectively. The initial diffusive clearance values of urea, creatinine, $Na^+$, and $K^+$ were calculated as 0.241, 0.241, 0.19, and 0.186 L/min, respectively from the $Q_{bi}$ (blood flow rate) value of 0.3 L/min, $Q_{di}$ (dialysate flow rate) value of 0.5 L/min, and $K_u$ (urea mass transfer coefficient) value of 0.77 L/min. Fig. 6, 7 and 8 showed the urea and creatine variations in intracellular and extracellular compartments for 4 hours hemodialysis treatment and 1 hour observation assuming the clearance rate of the solutes as 0.241 L/min.

These figures also represented the case of hyponatric dialysate, neutral dialysate and hypernatric dialysate, respectively. Both the intracellular and extracellular concentrations of urea were initially 13 mmol/L (80mg/dL in case of chronic hemodalysis patient) and creatine concentration were initially 5 mmol/L. The extracellular urea concentrations decreased below 3 mmol/L while the extracellular creatine concentration decreased lower than 1.5 mmol/L. The extracellular concentrations of urea and creatine were rebounded to 0.5mmol/L and 0.25mmol/L for concentration balance

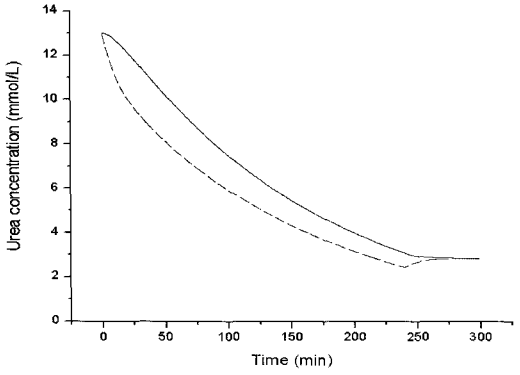


(a)

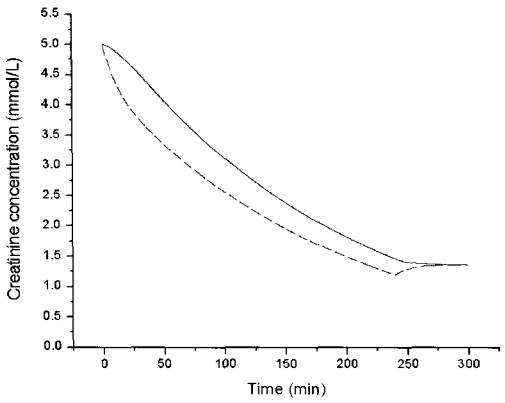


(b)

Figure 7 Time courses of Urea (a) and creatinine (b) concentratration during 4 hour hemodialyls treatment and 1 hour for observation (neutral dialysate : 140 mEq/L of both dialysate and plasma Na+ concentration)

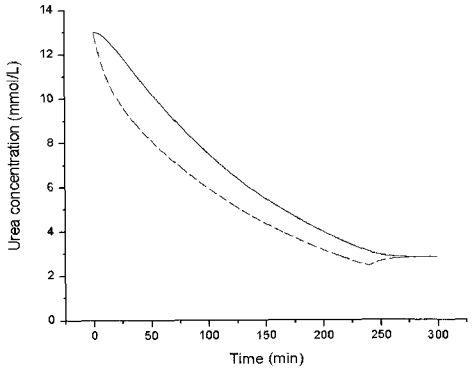


(a)

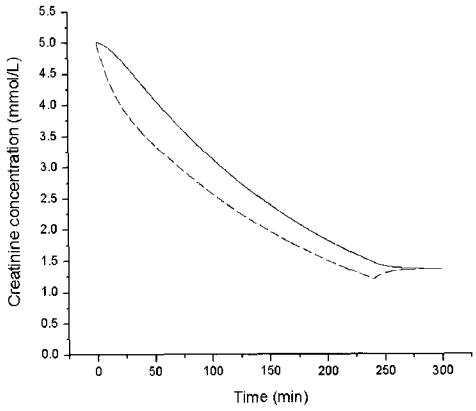


(b)

Figure 8 Time courses of Urea (a) and creatinine (b) concentratration during 4 hour hemodialyls treatment and 1 hour for observation (hyponatric dialysate: 150 mEq/L of dialysate Na+ concentration and 140 mEq/L of plasma Na+ concentration )

between intrcellular and extracellular pool. The patterns of plasma urea concentration naturally do not differ significantly among the cases of hyponatric, neutral and hypernatric dialysate. Fig. 9 showed the intrdialytic curves of plasma sodium concentration for 4 hour hemodialysis treatment and 1 hour observation predicted by the model with different sodium dialysate concentration (hyponatric, neutral and hypernatric dialysate).

In the hypernatric dialysate, the sodium concentration in plasma increased moderately and decreases immediately after the treatment. The plasma concentration in sodium decreased below the dialysate sodium concentration and continuously decreased even after the treatment in the neutral dialysate. Fig 10 represented the time courses of potassium concentration for 4 hours hemodialylsis treatment and 3 hours observation with different sodium dialysate.

The potassium concentration in plasma was not significantly varied for the three cases. It was lowest in the case of the hyponatric dialysate treatment. The time patterns of the capillary filtration rate and vascular refilling rate are shown in Fig. 12 for 4 hours hemodialysis treatment and 4 hours observation with different sodium concentrations in dialysate (hyponatric, neutral and hypernatric dialysate).

The capillary filtration rate is highest in the treatment of the hyponatric dialysate and lowest for the hypernatric dialysate. On the other hand, the vascular refilling rate is highest for the hypernatric dialysate and lowest for the hyponatric dialysate. Total extracellular osmolarity pattern indicated that it is highest for the hypernatric dialysate and lowest for the hyponatric dialysate (Fig. 13).

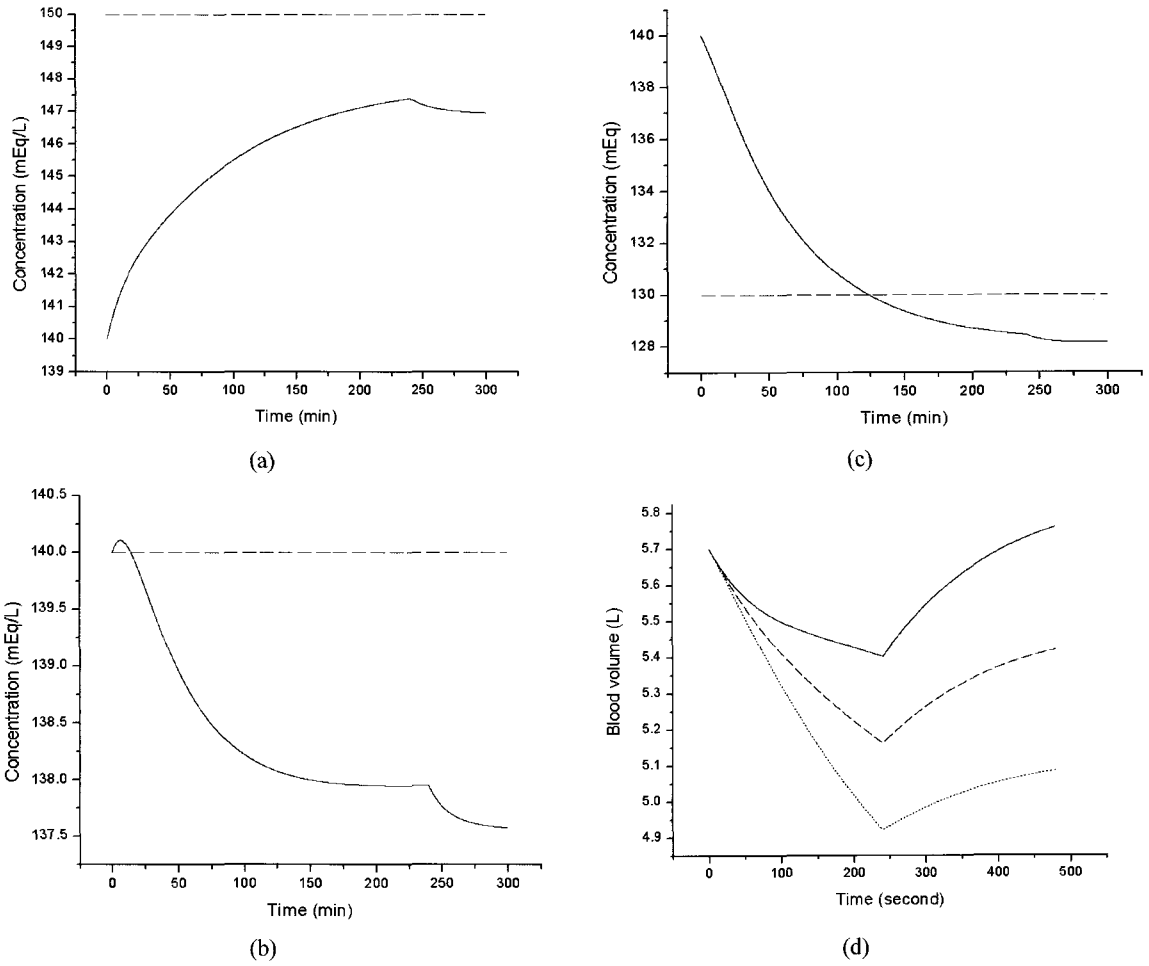


Figure 9 Time courses of extracellular sodium concentratration with hypernatric (a), neutral (b) and hyponatric (c) dialysate during 4 hour standard hemodialyls treatment and 1 hour for observation. Blood volume profile (d) during 4

The extracellular to intracellular volume ratio for 4 hour hemodialysis treatment was represented in Fig. 14, showing higher value for the hypernatric dialysate and lowest for the hyponatric dialysate.

## Simulation of Cardiovascular Response During Hemodialysis

Fig. 15 shows the time patterns of heart rate changes by baroreflex control according to the sodium dialysate concentration.

Heart rate increase during hemodialysis treatment induced blood volume decrease with a highest value for the hyponatric dialysate and lowest for the hypernatric dialysate. Left and right ventricular systolic compliances by baroreflex control were shown in Fig. 16. Fig. 17 shows time courses of kidney, lower limb, splanchnic and upper body resistance changes by baroreflex system during during 4 hour hemodialys treatment and 4hours for observation with different sodium dialysate concentration. All peripheral resistances increased during hemodialysis and decreased after the treatment.

## Discussion

In the present work, a mathematical model of the hemodialysis system (3 lumped body fluid model and 2 lumped solute kinetic model) coupled with the cardiovascular system (12 lumped parameter model) was developed to search for a rational choice of sodium concentration in dialysate that can prevent symptomatic hypotension and disequilibrium syndrome. The fluid shift between the intrcellular and extracellular pools, hence sodium concentration time pattern, also depends on the concentration of other solutes (such as $K^+$, Urea, Creatinine, etc) in the extracellular fluid and in the dialysate (Fig. 9). It was shown that sodium removal induced the decrease in the plasma sodium concentration

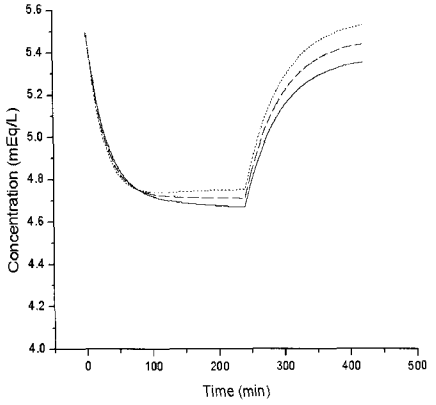


Figure 10 Time courses of potassium concentratration during 4 hours hemodialylsis treatment and 3 hours observation with different sodium dialysate (straight line : hypnatric dialysate, dashed line : neutral, dotted line : hypernatric dialysate, UF rate is 500mL/hr).

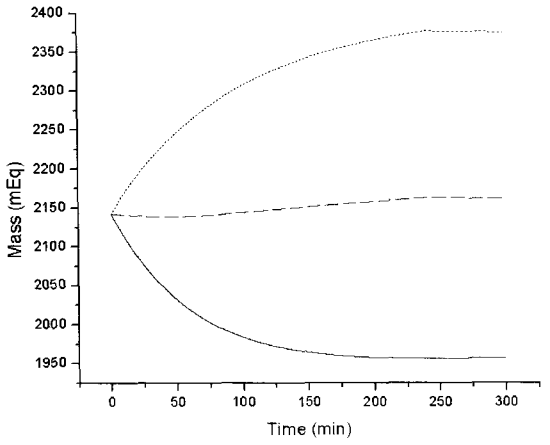


(a)

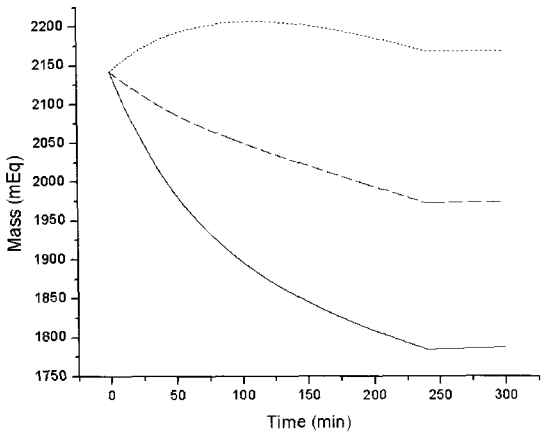


(b)

Figure 11 Time courses of total extracellular sodium mass during 4 hour standard hemodialysis treatment and 1 hour for observation without ultrafiltration (a) and with 500mL/hr of ultrafiltration (b) (straight line : hyponatric dialysate (130mEq), dashed line : sodium balance neutral (140mEq), dotted line : hypernatric dialysate (150mEq)).

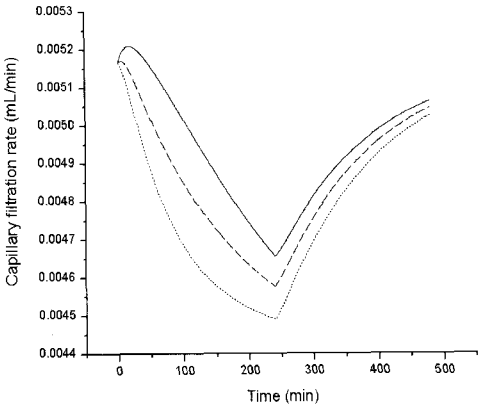


(a)

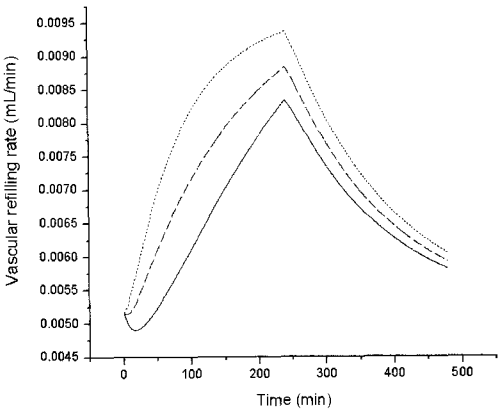


(b)

Figure 12 Time courses of capillary filtration rate (a) and vascular refilling rate (b) during 4 hour standard hemodialysis treatment and 4 hour for observation. (straight line : hyponatric dialysate (130mEq), dashed line : sodium balance neutral (140mEq), dotted line : hypernatric dialysate (150mEq)).

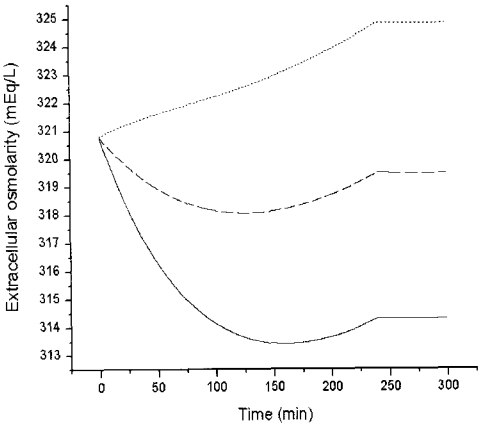


Figure 13 Time courses of total extracellular osmolarity during 4 hour standard hemodialysis treatment and 1 hour for observation. (straight line : hyponatric dialysate (130mEq), dashed line : sodium balance neutral (140mEq), dotted line : hypernatric dialysate (150mEq)).

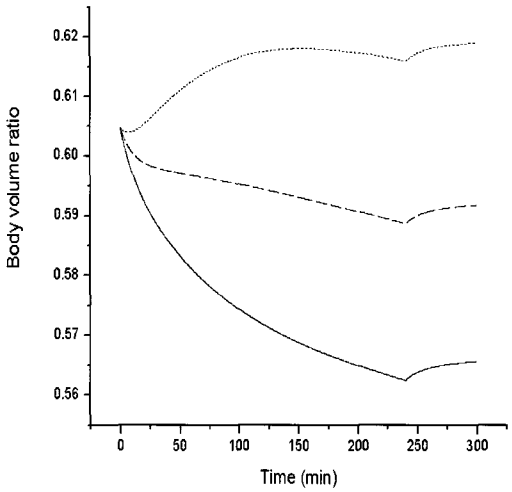


Figure 14 Time courses of extracellular to intracellular volume ratioduring 4 hour hemodialysis treatment and 1 hour for observation. (straight line : hyponatric dialysate (130mEq), dashed line : sodium balance neutral (140mEq), dotted line : hypernatric dialysate (150mEq)).

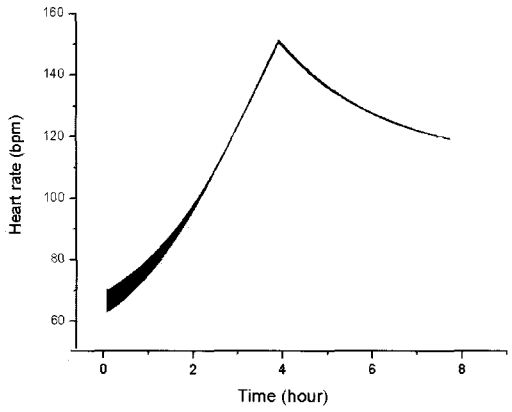


(a) Hyponatric

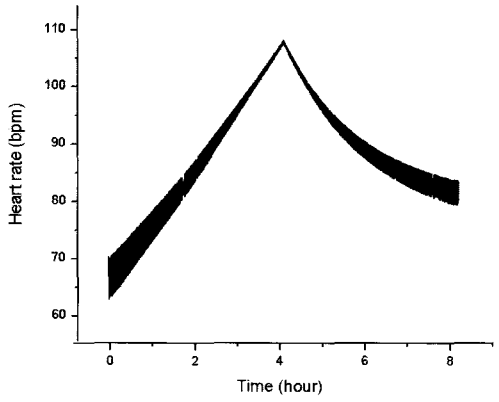


(b) Neutral

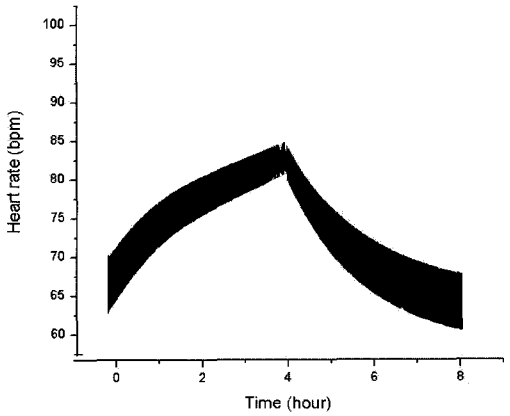


(c) Hypernatric

Figure 15 Time courses of heart rate changes by baroreflex systemduring 4 hour hemodialys treatment and 4hours for observation with different sodium dialysate concentration. (a : hyponatric dialysate, b : neutral dialysate , c : hypernatric dialysate)

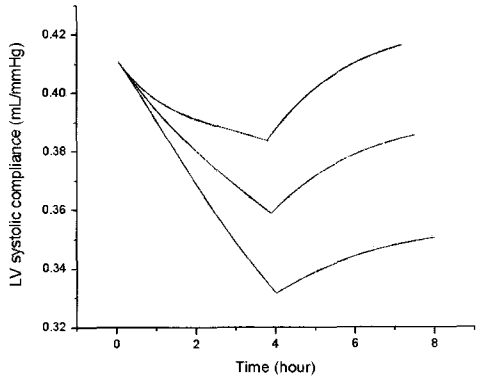


(a)

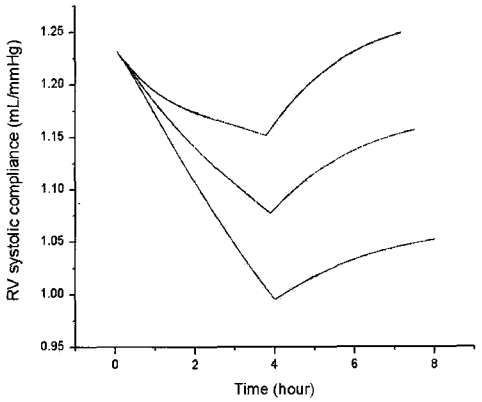


(b)

Figure 16 Time courses of left ventricular (a) and right ventricular (b) systolic compliance changes by baroreflex during 4 hour hemodialys treatment and 4hours for observation with different sodium dialysate concentration (straight line : hyponatric dialysate, dashed line : neutral dialysate , dotted line : hypernatric dialysate)

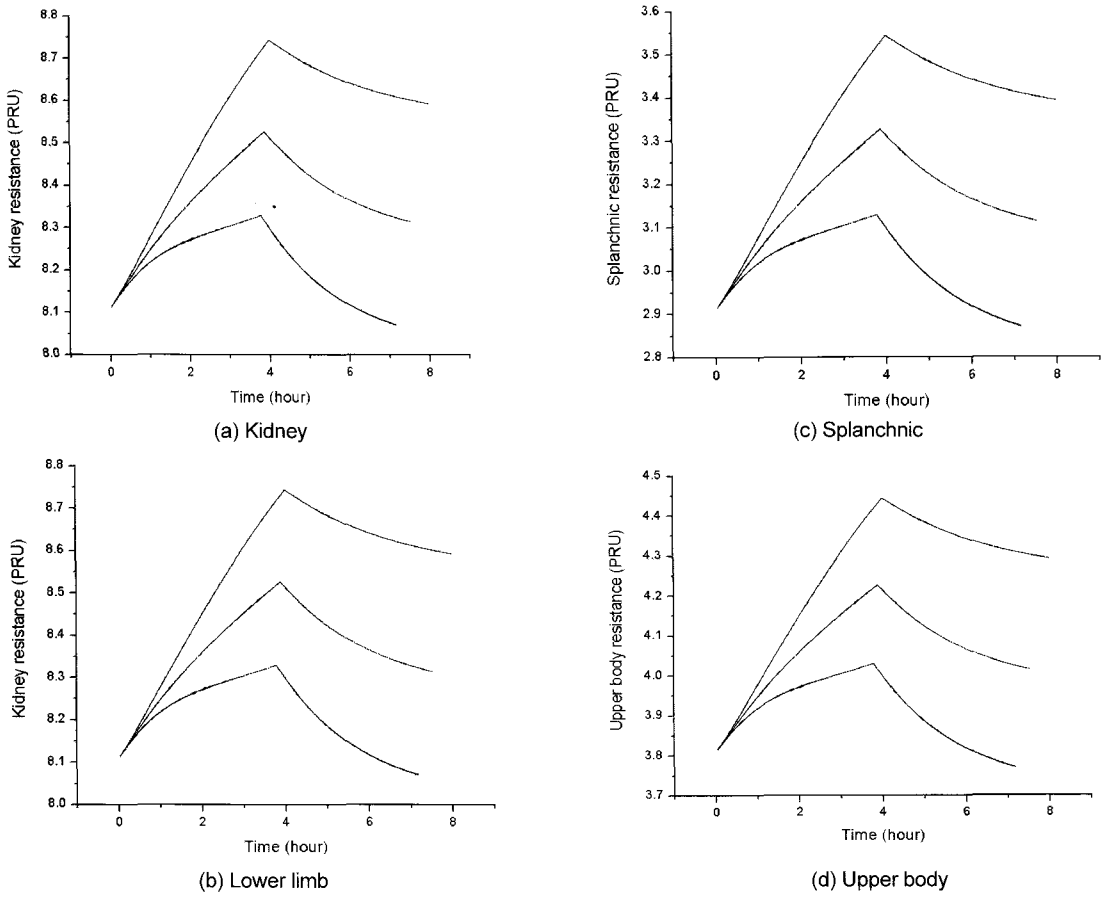


Figure 17 Time courses of peripheral resistance (a : kidney, b : lower limb, c : splanchnic d : upper body) changes by baroreflex system during during 4 hour hemodialys treatment and 4hours for observation with different sodium dialysate

whereas the increase of the plasma sodium concentration was augmented by the fluid volume loss from ultrafiltration. The decrease of plasma sodium concentration was induced by the flow shift from intracellular to extracellular space (Fig. 9(b) and (c)). The osmotic pressure and sodium removal by ultrafiltration (solvent drag phenomena) decreased the extracellular sodium concentration (Fig. 11).

When considering urea (Fig. 6, 7 and 8), its removal by diffusion exceeds the volume loss by ultrafiltration, thus causing a significant decrease in urea extracellular and intracellular concentration above all during the first half of the session. Since urea moves almost freely between the intracellular fluid (ICF) and extracellular fluid (ECF), its membrane permeability is 10 fold higher compared to that of sodium and urea. Differences in urea concentration between ICF and ECF are rapidly compensated for by transmembrane diffusion of urea and induce no fluid shift. Therefore, it is reasonable to state that the osmotic imbalance in dialysis is mainly induced by decreased sodium concentration and not by changes in urea concentration. Therefore, reduction in plasma osmolality can be minimized by modifying the sodium concentration in the dialysate according to the patient's plasma sodium concentration. Sodium concentratons in dialysate that are equal to or higher than those in the plasma prevent a decline in extracellular osmolality and inhibit intracellular water uptake (which predisposes the patient to disequilibrium).

In all the cases, capillary filtration rate decreased and vascular refilling rate increased during hemodialysis treatment because of higher interstitial fluid pressure than blood pressure at the arterial and higher oncotic pressure (that is osmotic pressure of proteins) in blood than in interstitial fluid (see Equation 6, 7 and Fig. 12). Finally, in the simulation of cardiovascular response to hemodialysis, heart rate and peripheral resistance increased and ventricular compliance and peripheral zero pressure filling volume decreased in order to compensate the dropped pressure due to blood volume

reduction during hemodialysis. By this kind of simulation study, we could predict cardiovascular response (heart rate, ventricular compliance and peripheral resistance) to hemodialysis and solute kinetics and body water balance during hemodialysis.

## Acknowledgments

This study was supported by 2003 Kangwon National University Grant (New Faculty Supporting Fund) and also supported by a grant of the Korea Health 21 R&D Project, Ministry of Health & Welfare, Republic of Korea. (HMP-02-PJ3-PG6-EV09-0001).

## References

1. Henrich WL, Woodard TD, Blachley JD, Gomez-Sanchez C, Pettinger W, Cronin RE: Role of osmolality in blood pressure stability after dialysis and ultrafiltration. Kidney Int 1980; 18 : 480~488.
2. Sargent JA, Gotch FA: Principles and biophysics of dialysis. Replacement of Renal Function by Dialysis. Ed. By John F.Maher: 3rd ed 1989; 87~143.
3. Davis TL: Teaching physiology through interactive simulation of hemodynamics (master's thesis). Cambridge, MA : Massachusetts instate of technology 1991.
4. Davis TL, Mark RG: Teaching physiology through simulation of hemodynamics. Comput Cardiol 1990; 17 : 649~652.
5. DeBoer RW, Karemaker JM: Hemodynamic fluctuations and baroreflex sensitivity in human: a beat-to-beat model. J Appl Physiol 1987; 253 : 680~689.
6. Sargent JA, Gotch FA: Mathematical modeling of dialysis therapy. Kidney Int 1980; 18(suppl 10) : 2~10.
7. Ursino M: Modeling Arterial Hypotension During Hemodialysis. Artificial Organs 1997; 21(8) : 873~890.
8. Ursino M: Prediction of Solute Kinetics, Acid-Base Status, and Blood Volume Changes During Profiled Hemodialysis. Annals of Biomedical Engineering 2000; 28 : 204~216.
9. Ziolko M, Pietrzyk JA, Grabska-Chrzastowska J: Accuracy of hemodialysis modeling. Kidney Int 2000; 77 (3): 1152~1163.
10. Akcahuseyin E, Nette RW, Vincent HH, van Duyl WA, Krepel H, Weimar W, Zietse R: Simulation study of the intercompartmental fluid shifts during hemodialysis. ASIO 2000; 46 (1) : 81~94.
11. Boyers DG, Cuthbertson JG, and Luetscher JA: Simulation of the human cardiovascular system: a model with normal response to change imposture, blood loss, transfusion, and autonomic blockade. Simulation 1972; 18 : 197~205.
12. Croston RC, Fitzjerrell DG: Cardiovascular model for the simulation of exercise, lower body negative pressure, and tilt table experiments. Proc 5th Ann Pittsburgh Conf Modeling Simulation 1974; 471~476.
13. Heldt T, Shim EB, Kamm RD, Mark RG: Computational modeling of cardiovascular response to orthostatic stress. J. Appl. Physiol. 2002; 92: 1239~1254.